Self-Organizing Sensory-Motor Map for Low-Level Touch Reactions

Philipp Mittendorfer and Gordon Cheng

***Abstract*— In this paper, we present a new method to automatically transfer touch stimulation into controllable, reflex reactions for articulated robots – such as a humanoid robot. Our work has been motivated by the necessity to automate the reaction setup for an increasing number of our multi-modal artificial sensor skin units (HEX-O-SKIN). Our method therefore evaluates the effect of isolated, sinusoidal degree of freedom (DoF) movements, around a current pose of the robot, towards the motion of each sensor unit. We do this by exploiting data from a 3-axis accelerometer – one of the multiple modalities located on every of our sensor units (SU). Direction and amplitude from all three axes enable us to generate signed weights, one per DoF and SU, leading to the partial construction of a sensory-motor map. In this paper, we focus on reactions towards lateral sensory modalities – such as a distance sensor. A higher acceleration along the surface normal thus leads to a higher lateral weight, while unwanted sideway movements decrease it. We then define a reaction controller at the level of each sensor unit. The sensory-motor map is used to map these local reactions, from units distributed all over the robot, into the robot's motor space. Through activation, inhibition or inversion it is possible to adapt these low-level controller instances to a given context. Here, we show experiments with a KUKA lightweight robotic arm reacting evasively or aggressively towards contact with a lateral distance sensor, emulating the sensation of light touch. In comparison to other related works, our method does not suffer from occlusion, complex touch situations or long calibration time.**

I. INTRODUCTION

A. Motivation

Human skin provides numerous inspirations for robots, deploying high resolution, multi-modal sensitivity over the whole surface. In comparison to a robot purely relying on joint information (position and/or force), a robot equipped with skin has a much richer information set. Human, with a set of roughly 5 million skin receptors, is not only able to classify different touch events, e.g. temperature changes or impacts, but can also accurately localize the origin of the sensation in a multi-touch situation and act meaningfully. In order to do so, integrative control algorithms need sensory-motor knowledge. Manually providing this information is not feasible, due to the possible high number of sensor units and degrees of freedom. To overcome this, automated calibration routines can be realized on robots equipped with artificial skins – the robot uses its own sensors to learn about itself. This is especially interesting when an artificial sensor skin is not designed for a single robot, but applicable across multiple robotic systems. An autonomous, fast re-calibration mechanism is also useful to accommodate hardware failure.

Philipp Mittendorfer and Gordon Cheng are with the Institute for Cognitive Systems, Technische Universität München, Karlstrasse 45/II, 80333 Munich, Germany Email: see http://www.ics.ei.tum.de/

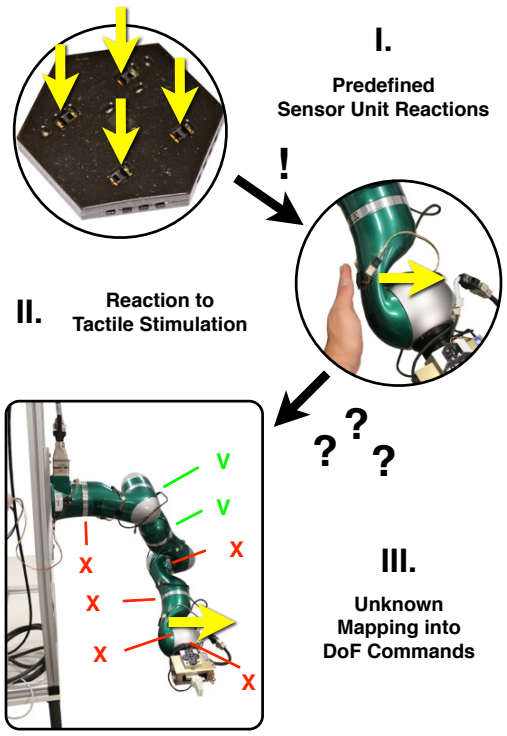

Fig. 1. Problem set - How could a robot directly actuate its degrees of freedom (DoF) in order to evade a touch with this skin senor unit (SU)? Potential DoF candidates to shift the sensor position along its surface normal are highlighted in green (V), others in red (X). In this paper, we will show an automated approach to resolve this issue in an effective manner; for lateral sensor modalities on a network of SUs, distributed on an articulated robot with multiple rotatory DoFs.

Different methods of self-exploratory learning have been reported in simulations, as well as in practical implementations. One approach in simulation is spatio-temporal correlation, learning topographic sensor structures from more or less random input [1]. Other simulated systems purposively seek contact with known external objects [2] or known body parts [3] to probe the sensor locations. In [4] topographic structures are used to classify interactive scenarios, like hugging or hand-shaking of human with a real robot, but the system gains no information about its motor-space. In [5], a cross-modal map is learned among joint, vision, and tactile sensory spaces, associating different pairs of sensor values when they are activated simultaneously. When no visual input is available, e.g. occlusion, this learning method can not interpret the given situation. Visual input can also

be used to learn the forward and inverse kinematic model of a robotic manipulator. Such as with the work of Lopes et al [6]. What they refer to as sensory-motor map is a function approximation in between a marker position in camera coordinates, an additional null space motion and the motor commands for a redundant robot.

The very nature of skin is to gather large amounts of multi-modal sensations from all over the body. Although, it is not necessary to take all these sensations into account on the highest level, it is still desirable to evaluate and react on every touch event. Human object manipulation is a good example for this – while we focus on manipulating a difficult object, we can at the same time maintain a steady contact with our environment and react on unexpected tactile input without loosing our major focus. This implies that multiple regulation mechanisms are in place to accomplish such complex tasks – the lowest level taking into account every sensation, whereas higher levels focus on specific preprocessed sensations.

In [4], tactile sensor data has been used to classify types of interaction, while in [7] tactile sensation helps the coach to provide direct corrections to the learning robot. Contact control makes it easier for robots to lift large objects [8], to center the load on carrying objects [9] or to detect slip during manipulation [10]. Instantaneous movements in response to a sensory stimulus must not only be limited to touch triggered reflexes for safer robots like, as in [11] and [12]. This type of behavior has also been used for interactive real-time guidance [13] and reflective grasping [14]. In [15], Nakamura et al. demonstrate the effectiveness of coaching the mapping in between preprocessed sensor information and predefined behavior primitives on grasping different objects.

Here we were motivated by our artificial skin sensor units (HEX-O-SKIN) reacting to multi-modal tactile stimuli [16]. In our previous work, we already issued a controller at the level of the sensor units, but resourced to manually providing the system with the appropriate reaction for every single sensor unit. As appropriate reaction, we fed a constant translational velocity vector to the inverse kinematic algorithm of the segment the sensor was mounted on. Here we were motivated to find a way to automatically map reactions from sensor to actuator space, as well as to provide a high level interface to adapt the low level controller from a higher level context.

B. New Approach

Our aim is to automatically map multi-modal touch stimuli with an artificial sensor skin, into controllable, reflex like reactions with the degrees of freedom (DoF) of an articulated robot – such as a humanoid robot. Therefore, we define instantaneous, low-level motion reactions towards multi-modal tactile stimulation on the level of a single sensor unit (SU). We then instantiate this behavior as many times as there are SUs distributed on the robot. In order to support future context driven high level controller, every controller instance features a standard interface to activate, inhibit or inverse reactions of a certain modality. The overall reaction of a SU is then mapped into DoF space using weights from a construct we refer to as a *sensory-motor map*. The sensory-motor map is organized in tiles, which are directly linked to poses of the robot (DoF positions). Tiles can be generated during an initial phase, to supply a set of key poses, or on demand, switching from reaction to exploration state. When there is no tile available for the current pose, our algorithm automatically selects the tile with minimal euclidean distance to the actual pose. Every tile contains a set of signed weights for every SU to directly transfer a SU reaction into DoF motions. In order to acquire the weights of a tile, for a pose, our algorithm applies motion pattern to all DoFs, one after the other. The algorithm then evaluates the effects each DoF had on the motion of every sensor unit. It does this by utilizing data from a 3-axis accelerometer, one of the multiple modalities available on every of our SUs. The direction and amplitude of the three axis responses enable us to generate signed weights, one per DoF and SU. In this paper, we focus on lateral sensor modalities only – such as a distance sensor, emulating the sensation of light touch. Thus, we generate only a single translational weight in the direction of the surface normal, which we continue to call lateral weight. A high acceleration along the surface normal increases this lateral weight, while unwanted sideway movements decrease it. Switching the direction from evaluation to reaction, only DoFs with a high contribution to a lateral motion of the SU will be actuated, when the connected controller instance launches a reflective action. This theory can easily be enhanced to also support other translational directions – e.g. x/y shearing. The advantage of our approach is that we require only minimal a-priori knowledge on how to control the degrees of freedom and read from the sensor units. Only few constraints have to be taken into account during the acquisition of the map – a fixed robot base/torso and a sufficient, unconstrained DoF motion range around every pose to be explored. We use an internal observer and are thus not limited by occlusion or any external components. Due to the touch-less approach, our method is able to acquire the information in a very short time, which is especially useful for ongoing re-calibration.

II. SYSTEM DESCRIPTION

In this section, we first introduce the theory of operation of our approach. We then describe how we assemble a sensory-motor map based on the accelerometer readings and show how we use this map to transfer reactions from other modalities like the distance sensor into motor space. Finally we give an overview of the hardware we used in our experiments.

A. Theory of Operation

1) **Working Principles:** Our new approach (refer to I-B) is based on three theorems: 1) Every sensor modality on our sensor unit has a preferred direction in which motion increases or decreases the sensor excitation; 2) The robot has an explicit central point in the kinematic tree towards which it is acting on reflex like, immediate reactions; 3)

Reactions from different sensor modalities and locations can be meaningfully super posed.

The first theorem implies that we can make use of the motion sensor on every of our sensor units, in order to evaluate appropriate reactions and transfer these to other modalities. To do so, it is necessary to know the alignment in between the new sensor modality and the motion sensor, which we precisely do with our sensor units (SU). The second makes it possible to reuse once explored sensory-motor weights for the same or sufficiently close poses. Since we use a motion sensor to evaluate reactions, it is necessary that the central point is nearly static during pose explorations. Only then, it is possible to extract the motion generated by a DoF from the sensor data, without any prior knowledge of the robot kinematics and the location/orientation of the sensor units. With a robotic arm, this central point is given by the part the robot is mounted to the environment. For a humanoid robot, we would have to artificially provide the point during pose explorations. This could for example be achieved by fixing the torso or hip in a calibration stand. The third theorem, makes it possible to sum all reactions of the different sensor modalities on a single unit before mapping this combined reaction to DoF actions. The resulting DoF commands of multiple SUs can then also be summed up. This statement is difficult, since with instantaneous reactions coming from more than one modality and/or sensor unit at a time, the DoF commands automatically interfere with each other in a positive or negative way. On evading a heat source one could for example impact with a wall, which itself triggers proximity and vibration reactions. These negatively seen chain reactions are normally not wanted. In a positive setting, a local slip detection could trigger a tighter contact of which the absolute strength is limited by force pain or task constrained, adapted limits. The appropriate quality and quantity of low level-reactions thus largely depends on the context. Here, we only propose a standard interface per sensor unit for a higher level controller.

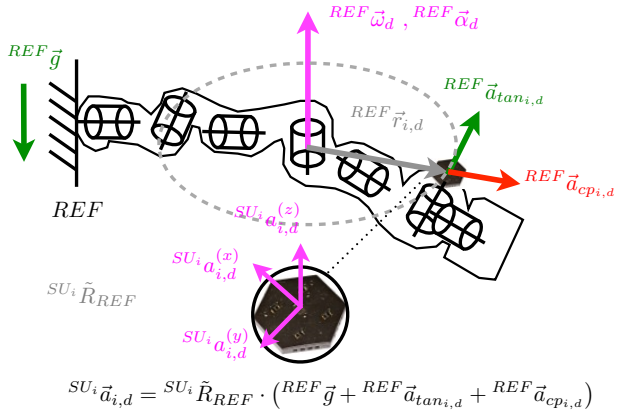

Fig. 2. Acceleration reading $^{SU_i}\vec{a}_{i,d}$ of an artificial sensor skin unit (SU) i due to the change $^{REF}\vec{\alpha}_d$ and value $^{REF}\vec{\omega}_d$ of velocity of a rotatory degree of freedom (DoF) d and additional gravity $^{REF}\vec{g}$. The position vector $^{REF}\vec{r}_{i,d}$ is in between the DoF axis d and the accelerometer center i. $^{SU_i}\tilde{R}_{REF}$ describes the current relative orientation of the SU accelerometer coordinate system i towards the reference (REF).

2) **Physical Formulation:** In Fig. 2 we show a simplified model of a single sensor unit (SU) mounted on an intermediate segment of a robotic arm with multiple derees of freedom (DoF) and a fixed base. As described in section I-B and II-A.1, we utilize the motion sensor on every sensor unit in order to find appropriate DoF velocity commands for other modalities on the same unit – e.g. contact with a distance sensor. We therefore evaluate the influence every DoF d has got on the direction and amplitude of motion of a unit i. Here, we provide a description of the effects every motion sensor is exposed to during exploration, given our constraint of a static central point is fulfilled (refer to II-A.1).

Neglecting skin deformations, and given rigid or quasi-rigid segments, every SU follows the acceleration of its mounting point. With a static reference segment like in Fig. 2, the acceleration of all mounting points can be directly controlled by actuating the related DoFs. Here, we only focus on ideal revolute DoFs with a velocity control interface. Although prismatic DoFs are easier to cope with our method, they directly produce motions that fit the accelerometer, revolute DoFs are more common with humanoid robots. A change in velocity $\frac{d}{dt}{}^{REF}\vec{\omega}_d(t) = {}^{REF}\vec{\alpha}_d(t)$ of a revolute DoF d has a direct influence on the acceleration of SU i, which composes from three different effects:
(1) The tangential acceleration $^{REF}\vec{a}_{tan_{i,d}}$, which is dependent on the rotatory acceleration of the DoF $^{REF}\vec{\alpha_d}$ and the vector $^{REF}\vec{r}_{i,d}$, in between the DoF axis d and the mounting point of SU i:

$$^{REF}\vec{a}_{tan_{i,d}} = {}^{REF}\vec{\alpha_d} \times {}^{REF}\vec{r}_{i,d} \tag{1}$$

(2) The centripetal acceleration $^{REF}\vec{a}_{cp_{i,d}}$, which is dependent on the angular velocity $^{REF}\vec{\omega_d}$ as well as the vector $^{REF}\vec{r}_{i,d}$:

$$^{REF}\vec{a}_{cp_{i,d}} = {}^{REF}\vec{\omega_d} \times ({}^{REF}\vec{\omega_d} \times {}^{REF}\vec{r}_{i,d}) \tag{2}$$

(3) And the gravity vector $^{REF}\vec{g}$.

In order to generate weights for the tiles of a sensory-motor map we maximize motion control in the desired direction, while minimizing motion in the others. Only the tangential acceleration $^{REF}\vec{a}_{tan_{i,d}}$ can be used, since this acceleration is directly controllable through changing the DoF velocity $^{REF}\vec{\omega}_d(t)$. We thus optimize the following weight generation (see II-B) towards the tangential acceleration. Even when the sensor could exclusively sense the tangential acceleration, the accelerometer would still sense a version $^{SU_i}\vec{a}_{tan_{i,d}}$ dependent on the relative orientation $^{SU_i}\tilde{R}_{REF}$ (see Fig. 2). This orientation is, like the vector $^{REF}\vec{r}_{i,d}$, dependent on the configuration and current pose of the robot, as well as the mounting (location/orientation) of the sensor unit. This is why we must explore every pose we wish to induce reactions in, when there is no prior knowledge about the sequential kinematic model. But, since $^{SU_i}\tilde{R}_{REF}$ and $^{REF}\vec{r}_{i,d}$ are smoothly dependent on the current DoF positions, a tile of a comparably close pose will still behave well.

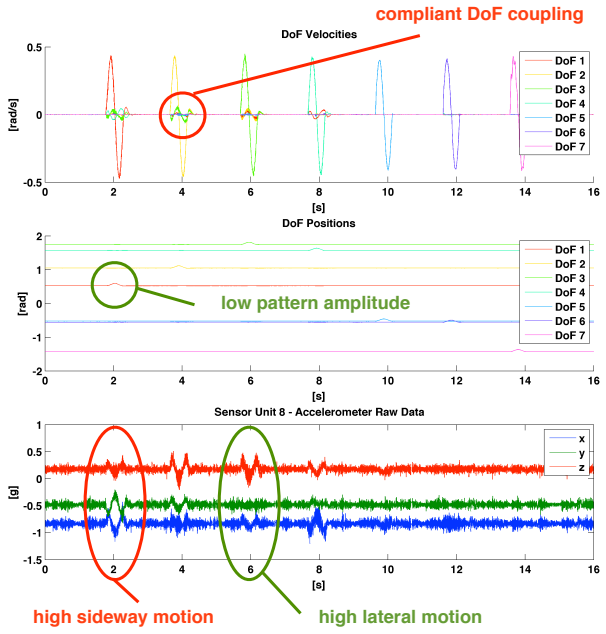

Fig. 3. Data from exploration of pose I, shown in Fig. 8 – The first graph shows the velocity pattern the robot performs on every degree of freedom (DoF), one after the other. The highlighted area shows high compliant coupling of DoFs due to the dynamics of the distributed mass. The second graph shows the angular DoF positions during exploration of pose I. The pattern amplitude is low and every DoF returns to its initial position. The last graph shows unfiltered accelerometer data from sensor unit (SU) with ID 8. The highlighted accelerometer readings explain the generation of a high lateral weight for DoF with ID 3, but a low one for DoF with ID 1. The readings show high z and low x/y activity for DoF with ID 3 and lower z and high x/y activity for DoF with ID 1. The surface normal of every sensor unit is aligned with the z axis of the accelerometer.

B. Generation of Sensory-Motor Map

1) **DoF Pattern Generation:** In order to automatically acquire the influence of a degree of freedom (DoF) d on the motion of a sensor unit (SU) i for a given pose, it is necessary for the robot to apply isolated motion pattern to all of its DoF, one after the other. It is important to only move one DoF at a time in order to be able to directly separate the information. We utilize an accelerometer in order to evaluate the influence of a DoF motion towards the motion of a sensor unit (see I-B). Consequently the robot has to generate motion pattern which the sensor is able to measure. In section II-A.2, we explained why we want to maximize the influence of the tangential acceleration ${}^{SU_i}\vec{a}_{tan_{i,d}}$, while minimizing side effects like the centripetal acceleration ${}^{SU_i}\vec{a}_{cp_{i,d}}$ and the rotation of the gravity vector ${}^{SU_i}\vec{g}$. The centripetal acceleration can be minimized by keeping the angular DoF velocity ω_d low. The influenced of the rotated gravity vector is constant and thus subtract-able when the DoF motion only covers a small angular range $\triangle\varphi_d$. In order to maximize the tangential acceleration, the angular acceleration α_d has to be high. With compliant robots and in order to avoid oscillations, it is advisable to smooth the commanded angular velocity $\omega_d(t)$ as well as the induced acceleration $\alpha_d(t)$ and jerk $\frac{d}{dt}\alpha_d(t)$. At the same time we need to return to the same DoF position $\varphi_d(0) = \varphi_d(T)$ once the exploration pattern with length T stops on the current DoF and is shifted to the next DoF. One possible velocity pattern $\omega_d(t)$ that fulfills all these requirement is a sine wave:

$$\omega_d(t) = Asin(2\pi ft) \tag{3}$$

Of which the deviated acceleration pattern $\alpha_d(t)$ is:

$$\alpha_d(t) = 2\pi fAcos(2\pi ft) \tag{4}$$

One integral of the velocity pattern is the position $\varphi_d(t)$:

$$\varphi_d(t) = \frac{A}{2\pi f}(1 - cos(2\pi ft)) \tag{5}$$

All together these equations give us a guideline how to dimension the DoF exploration pattern. The selection of A is limited by the maximum DoF velocity oft the robot and the tolerable influence of the centripetal acceleration. $2\pi fA$ has to be lower than the maximum DoF acceleration and below a value that shows excessive coupling between the DoFs due to the distributed mass. $\frac{A}{2\pi f}$ has to be small enough to be able to neglect the influence of the rotating gravity vector. Still $\alpha_d(t)$, and such $2\pi fA$, has to be sufficiently large so that the effect of a DoF pattern towards the measurement of the accelerometer ${}^{SU_i}\vec{a}_{i,d}$ stands out from the sensor noise. Since endless sinusoidal DoF pattern would not allow to switch the pattern between DoFs we additionally need a windowing function $F(t)$ so that $\omega_d(t) = Asin(2\pi ft) \cdot F(t)$ and its derivatives still meet the constraints.

2) **Weight Extraction:** As described in II-A, we need to extract lateral weights $w^z_{i,d,p}$ from the raw accelerometer records ${}^{SU_i}\vec{a}_{i,d,p}[n]$ of sensor unit with ID i on the generation of a sinusoidal pattern with DoF with ID d in the current pose with ID p. First, we subtract the mean value from every of the three axes in order to eliminate constant sensor offsets and the rotated gravity vector ${}^{SU_i}\vec{g}$ which is nearly constant for a well defined pattern (see II-B.1). We then apply a digital low pass filter with a bandwidth B larger than 10 times the pattern frequency f to eliminate noise and high frequency vibrations from the robot. This two stage approach is superior to a common bandpass due to the lower order and shorter sample set. On finding the maximum and minimum for every axis we can calculate the amplitude $\vec{A}_{i,d,p}$. In this paper, we place our focus only on reactions in the lateral direction. Thus, we only need the sign of the z-axis $s^z_{i,d,p}$ component, aligned with the surface normal. The sign is positive when the sampled wave form on the z-axis is out of phase with the excitation pattern and positive when it is in phase. In our experiments, we assumed the sign to be positive when half of the maximum is reached later than half of the minimum. Since we start every exploration pattern with a positive velocity on the DoF (see II-B.1) this leads to an evasive motion in the reaction phase. Finally, we can calculate the lateral weight from all components as follows:

$$w^z_{i,d,p} = s^z_{i,d,p} \cdot \frac{A^z_{i,d,p}}{A^x_{i,d,p} + A^y_{i,d,p} + A^z_{i,d,p}} \tag{6}$$

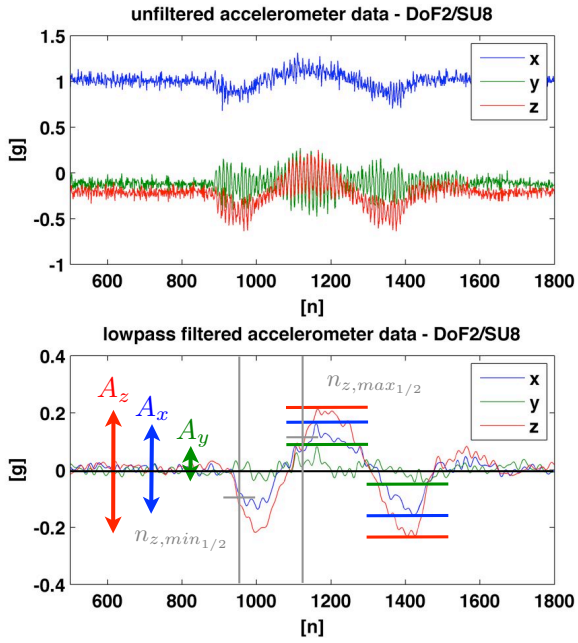

Fig. 4. Weight extraction from accelerometer data – The plots show unfiltered and filtered data from sensor unit with ID 8 on a pattern generated by degree of freedom with ID 2 in pose I (see Fig. 8). A_x, A_y and A_z constitute ideally of the maximal amplitude of the tangential acceleration $\vec{a}_{tan}$ (see Fig. 2). The first occurrence of the half of the minimum $n_{min,z_{1/2}}$ and the half of the maximum $n_{max,z_{1/2}}$ is a measure of the sign s (out of phase/in phase) in between motion generation and sensation.

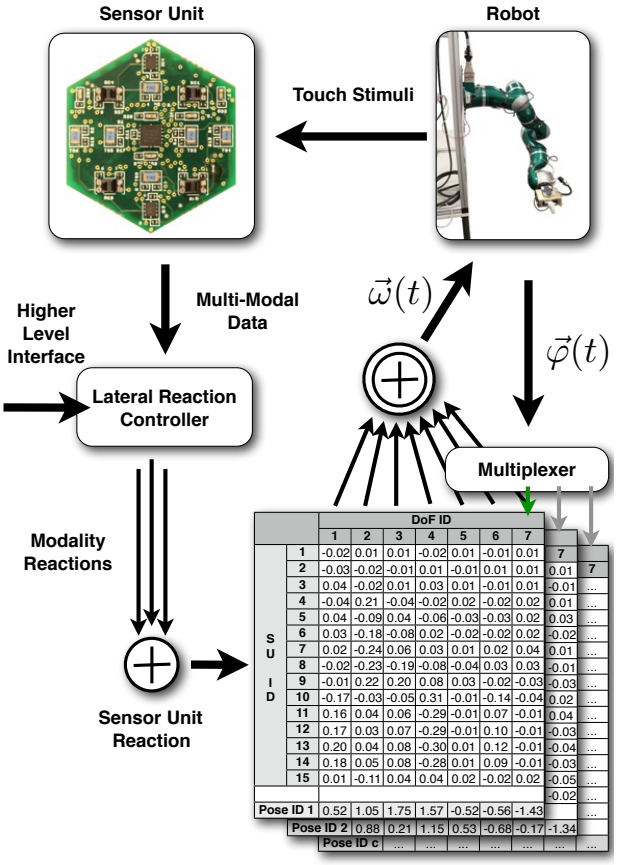

Fig. 5. Control loop of the reaction control system – Tactile stimulations are sensed by the multi-modal sensor units. A low-level controller instance evaluates the sensor input and provides an interface for a higher level controller. All reactions for a single sensor unit are super posed and then mapped by the according row of the sensory-motor map. A multiplexer automatically selects the part of the sensory motor map with the minimal euclidean distance to the current pose. Finally, all generated degree of freedom commands are super posed and sent to the robot.

Thus, a high lateral effect of a DoF pattern in the accelerometer readings increases the lateral weight, while effects in the other two shearing directions decrease it. This calculation is valid as long as the z-axis of the accelerometer is aligned with the surface normal (see II-A.1).

3) **Tile and Map Assembly:** Fig. 8 shows two assembled tiles for two different robot poses. A tile of the sensory motor map is in fact a table of weights per degree of freedom (DoF) and sensor unit (SU) with the dimension of number of SUs times the number of DoFs times the number of weights. With the current scope of our work, we focused only on one weight, the lateral weight $w^z_{i,d,p}$. Our approach can easily be extended to generate weights for all three translational directions. Additional to the weight matrix, it is also necessary to record the robot pose the weights have been sampled in. In essence, the *sensory motor map* is a stack of tiles as shown in Fig. 5 for multiple robot poses of which the robot can select one at a time in order to map reactions (see II-C).

C. Mapping of Multi-Modal Tactile Stimuli

1) **Multi-Modal Sensor Unit Reaction:** In order to react on tactile stimulations it is necessary to set up effective controller. As described in I-B, we can define and organize these controller on the level of the sensor units. In this paper, we focused on a single lateral sensor modality m and a lateral reaction $\rho^z_{i,m}$ – evading or seeking contact based on an active infrared short-distance sensor. In [16] we demonstrated that we can perform at least three kind of reactions: 1) impact vibrations; 2) contact proximity; and 3) temperature *chill* effects. Thus, the original problem is a many to few mapping. Here we decided to super pose all modality reactions on a single SU, while introducing weights to provide an interface for the next level controller. With a controllable weight $\psi^z_{i,m}$ per modality m, on a sensor unit i, it is already possible to activate, inhibit or inverse a SU modality reaction:

$$\rho^z_i = \sum_m \psi^z_{i,m} \cdot \rho^z_{i,m} \tag{7}$$

2) **Sensory-Motor Reaction Mapping:** Fig. 5 shows an overview of the control loop of our method. In reaction mode, our algorithm searches every $100ms$ for the best current tile in memory, in order to map sensor unit reactions with. The best fitting tile is currently selected by minimizing the euclidean distance in between the current position $\vec{\varphi}(t)$ of the DoFs and the vectors of DoF positions, which was memorized during the exploration of every tile. With an update rate of $1ms$ our algorithm then multiplies every

sensor unit weight vector $\vec{w}^z_{i,p}$ in the tile with the according super posed sensor unit reaction ρ^z_i. As there are normally more SUs then DoFs and every SU generates its own full desired velocity command vector $\vec{\omega}(t)$ it is again a many to few mapping. Here, we decided to super pose every DoF reaction with an equal weight:

$$\vec{\omega}(t) = \sum_i \vec{w}^z_{i,c} \cdot \rho^z_i \tag{8}$$

D. Hardware

In this subsection we provide an overview of the hardware we used for our implementation.

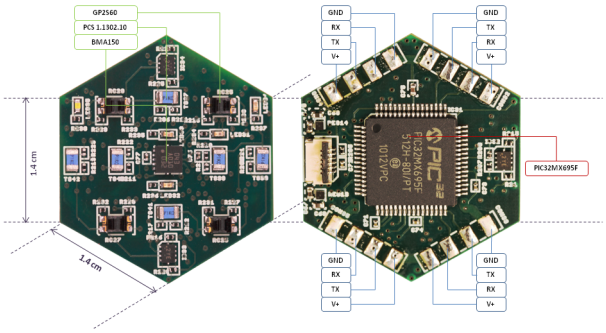

Fig. 6. HEX-O-SKIN sensor unit - The local controller and four combined data/power ports are visible on the back side. The front side features multiple sensor modalities – currently temperature, proximity and acceleration.

1) **HEX-O-SKIN:** What we refer to as HEX-O-SKIN sensor unit, is a rigid hexagonal PCB with multiple sensors on the front side and a local controller on the back. Each modality emulates parts of the human touch cues – e.g. temperature, vibration, light touch (see [16] for further details). Every sensor unit features 4 ports to directly connect it to its neighbors. Data is routed actively, power passively through a system of connected sensor units. The sensor units are placed next to each other in an elastomer mold, so that they are able to conform to the surface they are mounted on. We call such an organization entity skin patch of which at least one boundary port has to be connected to our custom PC interface, a *Tactile Section Unit* (TSU).

In this paper, we decided to make use of the 3-axis accelerometer available on every sensor unit, a BMA150 from BOSCH, as well as the proximity sensor, a GP2S60 from SHARP (see Fig. 6). The z-axis of the accelerometer is exactly aligned with surface normal of our sensor unit, which makes it perfect to sense motion in the direction of lateral sensors like the proximity sensor.

2) **Robot and Controller:** We evaluated our approach on a KUKA light weight robotic arm. This robot has 7 compliant joints with one degree of freedom per joint. The robot can be operated in a joint velocity command mode, which we used. All physical constraints, e.g. self-collision, are met within the robot controller.

III. EXPERIMENTS

In this section, experimental validation of our approach is presented.

A. Experimental Setup

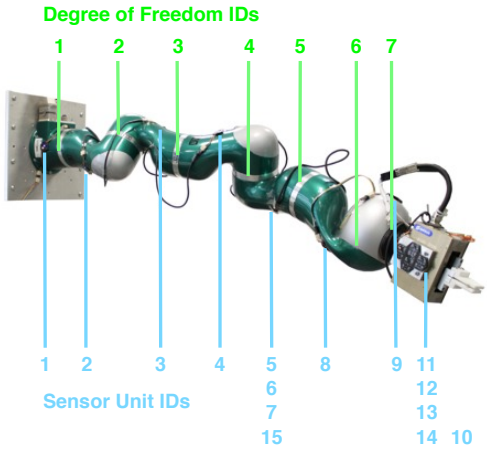

Fig. 7. Experimental setup - Distribution of sensor units (blue) and degrees of freedom (green) along the serial robotic chain. Not all sensor units are visible at a time – e.g. sensor unit with ID 10 is located on the opposite side of the four closely connected sensor units with ID 11-14, which directly face the reader.

In order to validate our approach we distributed 15 of our sensor units on a KUKA light weight robotic arm in a shoulder like configuration. Fig. 7 illustrates the distribution of sensor units and degrees of freedom along the serial robotic chain. Every degree of freedom and sensor unit is automatically allocated a unique identification number (ID), ranging from 1 to the maximum number of its type.

The generator for the sinusoidal DoF velocity pattern was set to an amplitude of $A = 0.4rad/s$ with a frequency of $f = 2Hz$ and a length of a single wave of $500ms$, cut by a rectangular window function $F(t)$. The acceleration recording of every SUs was started $500ms$ before the DoF pattern was released and stopped $500ms$ after the pattern was stopped.

We then detected touch by applying a threshold of 350 ticks on the infrared sensor raw data. This equals a human hand being closer than roughly $2mm$. The exited modality reaction strength ρ^z_i was set to 1, with a default control weight $\psi^z_{i,m}$ of 0.4. Consequently the excitation of every DoF by the controller instance is $0.4rad/s$ times the according lateral weight out of the currently selected tile.

B. Results

Fig. 8 shows two out of many poses we tested. Analyzing the weights for the sensor units with ID 11 to 14, one can easily recognizes the similarity of direction and amplitude of the generated lateral weights, although all weights in the map are generated independently. This must be as all four units are located closely and mounted with the same orientation on an even surface. All accelerometer coordinate systems of these units are thus aligned and, neglecting small deviations,

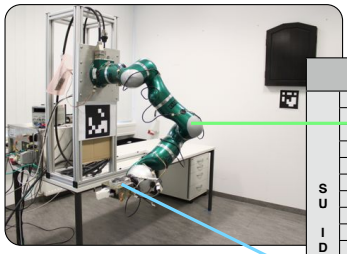

SUID	DoF ID 1	2	3	4	5	6	7
1	-0.02	0.01	0.01	-0.02	0.01	-0.01	0.01
2	-0.03	-0.02	-0.01	0.01	-0.01	0.01	0.01
3	0.04	-0.02	0.01	0.03	0.01	-0.01	0.01
4	-0.04	0.21	-0.04	-0.02	0.02	-0.02	0.02
5	0.04	-0.09	0.04	-0.06	-0.03	-0.03	0.02
6	0.03	-0.18	-0.08	0.02	-0.02	-0.02	0.02
7	0.02	-0.24	0.06	0.03	0.01	0.02	0.04
8	-0.02	-0.23	-0.19	-0.08	-0.04	0.03	0.03
9	-0.01	0.22	0.20	0.08	0.03	-0.02	-0.03
10	-0.17	-0.03	-0.05	0.31	-0.01	-0.14	-0.04
11	0.16	0.04	0.06	-0.29	-0.01	0.07	-0.01
12	0.17	0.03	0.07	-0.29	-0.01	0.10	-0.01
13	0.20	0.04	0.08	-0.30	0.01	0.12	-0.01
14	0.18	0.05	0.08	-0.28	0.01	0.09	-0.01
15	0.01	-0.11	0.04	0.04	0.02	-0.02	0.02
Pose	0.52	1.05	1.75	1.57	-0.52	-0.56	-1.43

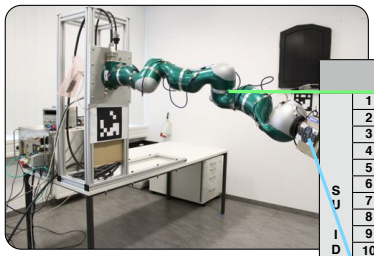

SUID	DoF ID 1	2	3	4	5	6	7
1	0.01	-0.02	-0.01	-0.02	-0.01	0.01	0.01
2	-0.02	0.03	-0.02	-0.02	0.02	0.01	-0.01
3	0.01	0.03	0.02	-0.03	0.01	-0.02	0.01
4	-0.04	0.19	-0.03	-0.04	0.02	-0.02	0.03
5	0.06	-0.34	0.04	-0.10	-0.03	-0.03	-0.02
6	0.04	-0.36	0.05	0.04	0.02	0.02	0.01
7	0.03	-0.28	0.04	0.03	0.02	-0.02	-0.01
8	-0.01	-0.09	0.06	-0.09	-0.02	0.02	-0.03
9	0.02	0.08	0.08	0.13	-0.02	-0.02	0.02
10	-0.18	-0.55	0.06	0.35	-0.05	-0.12	0.04
11	0.13	0.52	-0.04	-0.32	-0.05	0.07	-0.03
12	0.14	0.54	-0.04	-0.34	-0.05	0.08	-0.04
13	0.14	0.56	-0.05	-0.35	0.06	0.12	-0.03
14	0.14	0.56	-0.04	-0.33	-0.07	0.09	-0.05
15	0.04	-0.34	0.05	0.06	-0.03	0.02	-0.02
Pose	0.88	0.21	1.15	0.53	-0.68	-0.17	-1.34

Fig. 8. Resulting sensory-motor map – Two parts of the sensory motor map related to the displayed poses of the robot. Sensor units (SU) with ID 11-14, highlighted in blue, are located close to each other on the upper side of the box like framework of the gripper. Degree of freedom (DoF) with ID 4 is highlighted in green. DoF IDs are here counted up linearly from the base to the end effector of the KUKA robotic arm.

are subject to the same motion trajectory on a DoF pattern. Sensor unit with ID 10 always shows similar amplitudes compared to SUs with ID 11 to 14, but with an opposite sign. This is correct as the unit has been mounted on the opposite side of the box like framework of the robot's gripper, shifting the accelerometer coordinate system by 180 degrees. Touching the robot at sensor unit with ID 11-14 makes the robot evade the touch along the surface normal, the more SUs are simultaneously touched, the stronger is the reaction. This is due to the super posing behavior of the reaction controller (see II-C.2). Touching two opposite modules, e.g. sensor unit with ID 10 and 11, the behavior should ideally compensate each other. Practically there is minor DoF motion left due to inherent sensor noise, sensor offsets, small alignment mismatches and the already explained compliant coupling between multiple DoFs during pose exploration (see Fig. 3). Changing from pose I to pose II the weights for sensor units with ID 10 to 14 which are related to degree of freedom with ID 4 remain nearly the same, while in the second pose the weight of DoF with ID 2 gains a significant influence. For these sensor unit IDs a touch reaction in pose II is also stronger than in pose I due to the higher absolute of the lateral weight vector. This shows the influence posture changes have in the sensory motor map. We know that it is very easy to find appropriate inverse kinematic solutions on long, highly actuated kinematic chains but difficult on short, under-actuated ones. How good does our approach thus work for a short, under-actuated sensor unit location? One example is sensor unit with ID 4 located on the 4th segment with only 3 DoFs in between the mounting position and the robot base. Our algorithm found a high weight for DoF ID 2, which we could verify by touching the sensor unit. We then activated a "follow me" or "evade touch" scenario. On-line switching in between these two states is possible through our higher level interface. We showed this behavior to multiple human test candidates, with a human interacting with the robot. The overall reaction of a human seeing the robot reaction was positive and the motion considered appropriate.

Please also see our submitted video.

C. Discussion

Having a look at the generated weights in Fig. 8, it is quickly noticeable that there are small weights also for completely unrelated DoFs. This is partially due to coupling effects shown in Fig. 3. Another impact has the usage of a rectangular window function to generate time limited DoF pattern during exploration. Similar to the long exploration time per pose, roughly 12 seconds, we have not optimized our system yet. Another issue we expected but did not suppress yet is the miss-balance of reactions of SUs. This appears when one SU has a lot of high weights for most of the DoFs, while another has only few, small ones. An option could be to normalize the weight vector for every SU. Due to sensor noise and imperfections, it is then necessary to apply limits to the implicit amplification of small weights. Looking through the tables in Fig. 8 there are sensor units with only very small lateral weights for all degrees of freedom. In this case only an additional motion of the base could actuate the sensor unit appropriately. In contrast to our presented approach actuating the base, e.g. the torso of a humanoid robot requires sophisticated kinematic and environmental knowledge.

Another topic we would like to discuss here is the scalability of our solution with an increasing number of degrees of freedom and sensor units. Currently every sensor unit generates new data packages, containing all sensor data, at a fixed internal rate of $1kHz$, regardless if this data is used to evaluate or react. The computer has to be able to cope with the incoming amount of minimal size UDP packages and decode the data in real time. During a pose evaluation we sample a maximum of 2000 three dimensional acceleration values per sensor unit and DoF exploration pattern. Since we directly compute the weights after each DoF pattern the memory requirement scales linearly with the number of sensor units. The computational load for the weight calculation is minor (see II-B.2). A major scalability issue is the possible amount of DoF poses. Given a very rough discretization of the workspace of every DoF into four set points, it

would be necessary to evaluate the enormous number of $4^7 = 16384$ possible poses for the 7 DoF KUKA robotic arm. This shows the importance to: 1) Minimize the search space to interesting, task related poses only; 2) Enhance the approach with structural knowledge for complicated robots, e.g. a humanoid. With a humanoid robot we already proposed to center the touch reactions at the torso. Knowledge about the kinematic tree could help to decouple the search space of serial chains connected by the torso – e.g. left and right arm. Another scalability issue is the complexity of reaction controller. Here we decided to instantiate the same controller for every sensor unit. In order to keep the computational load and latency low, we only utilize simple proportional or switching mode controller.

IV. CONCLUSION

A. Summary

In this paper, we presented a self-contained method for articulated robots to automatically set up low-level reactions on lateral stimulation of our multi-modal artificial skin sensor unit. We experimentally demonstrated that we can make use of one of the sensor modalities on our sensor units – an accelerometer – to find appropriate actuator movements to react on tactile stimulation from other lateral modalities on the same unit. Through a sensory-motor map, combining exploration results for multiple robotic poses, we were able to transfer behaviors defined for a single sensor unit to all sensor units distributed on the robot. We then introduced our multi-modal tactile sensor units – HEX-O-SKIN – which was utilized in an experimental setup on a KUKA light weight robotic arm. With this experimental setup we presented results that support our method to automatically setup low level sensor-motor touch reactions.

B. Contribution

Our contribution is towards the facilitation of using large numbers of distributed sensor units on articulated robots – especially, artificial sensor skins. Our method provides parts of the body schema information within a very short time and applies only few controllable constraints. Starting from minimal a-priori information our system explores appropriate reactions on lateral tactile stimuli. Working at a hardware near level, our controller can directly react on new inputs, reducing the processing load at higher levels. The presented method works as an internal observer and thus does not suffer from occlusion like vision based systems or is in need of external components. We do not aim to substitute traditional learning algorithms but wish to facilitate and speed up the initial or re-calibration process for complex sensor actuator systems – like humanoid robots.

Acknowledgment

This work was supported (in part) by the DFG cluster of excellence 'Cognition for Technical systems CoTeSys'.

REFERENCES

[1] Y. Kuniyoshi, Y. Yorozu, Y. Ohmura, K. Terada, T. Otani, A. Nagakubo, and T. Yamamoto, "From humanoid embodiment to theory of mind," *Lecture Notes in Computer Science*, pp. 202–218, 2004.

[2] G. Cannata, S. Denei, and F. Mastrogiovanni, "Towards automated self-calibration of robot skin," May 2010, pp. 4849–4854.

[3] S. Fuke, M. Ogino, and M. Asada, "Body image constructed from motor and tactile images with visual information," *International Journal of Humanoid Robotics*, vol. 4, no. 2, pp. 347–364, March 2007.

[4] T. Noda, T. Miyashita, H. Ishiguro, and N. Hagita, "Map acquisition and classification of haptic interaction using cross correlation between distributed tactile sensors on the whole body surface," *IEEE International Conference on Intelligent Robots and Systems*, pp. 1099–1105, November 2007.

[5] Y. Yoshikawa, H. Kawanishi, M. Asada, and K. Hosoda, "Body scheme acquisition by cross modal map learning among tactile, visual, and proprioceptive spaces," *In Proceedings of the Second International Workshop on Epigenetic Robotics*, 2002.

[6] M. Lopes and J. Santos-Victor, "Learning sensory-motor maps for redundant robots," *International Conference on Intelligent Robots and Systems*, pp. 2670–2676, October 2006.

[7] B. D. Argall, E. L. Sauser, and A. G. Billard, "Policy adaptation through tactile correction," *Thirty Sixth Annual Convention of the Society for the Study of Artificial Intelligence and Simulation of Behaviour*, March 2010.

[8] Y. Ohmura and Y. Kuniyoshi, "Humanoid robot which can lift a 30kg box by whole body contact and tactile feedback," *International Conference on Intelligent Robots and Systems*, pp. 1136–1141, december 2007.

[9] T. Mukai, M. Onishi, T. Odashima, S. Hirano, and Z. Luo, "Development of the tactile sensor system of a human-interactive robot "riman"," *IEEE TRANSACTIONS ON ROBOTICS*, vol. 24, no. 2, pp. 505–512, april 2008.

[10] D. Göger, N. Gorges, and H. Wörn, "Tactile sensing for an anthropomorphic robotic hand - hardware and signal processing," *IEEE International Conference on Robotics and Automation*, pp. 895 – 901, 2009.

[11] T. S. Dahl and A. Palmer, "Touch-triggered protective reflexes for safer robots," *Proceedings of the International Symposium on New Frontiers in Human-Robot Interaction*, pp. 27–33, 2010.

[12] M. Battaglia, L. Blanchet, A. Kheddar, S. Kajita, and K. Yokoi, "Combining haptic sensing with safe interaction," *International Conference on Intelligent Robots and Systems*, pp. 231–236, 2009.

[13] V. J. Lumelsky, M. S. Shur, and S. Wagner, "Sensitive skin," *IEEE Sensors Journal*, vol. 1, pp. 41–51, 2001.

[14] P. A. Schmidt, E. Mael, and R. P. Wuertz, "A sensor for dynamic tactile information with applications in human-robot interaction and object exploration," *Robotics and Autonomous Systems*, vol. 54, pp. 1005–1014, December 2006.

[15] Y. Nakamura, T. Yamazaki, and N. Mizushima, "Synthesis, learning and abstraction of skills through parameterized smooth map from sensors to behaviors," *International Conference on Robotics and Automation*, pp. 2398–2405, May 1999.

[16] P. Mittendorfer and G. Cheng, "Humanoid multi-modal tactile sensing modules," *IEEE Transactions on Robotics*, vol. 27, no. 3, pp. 401–410, June 2011.